H_∞ Loop Shaping for Positioning Control System with Nonlinear Friction

M2011MM067 Yuki SUGIYAMA

Adviser: Isao TAKAMI

1 Introduction

1.1 Background

In general, for the precise positioning control, it is necessary to satisfy the specification which follows the reference without stationary error and overshoot. However, the friction property of the machine element deteriorates the positioning performance. The stick-slip motion, the stationary error, overshoots, and the limit cycles are generated as an influence of friction. To achieve the friction compensation, many methods are proposed such as disturbance observer[1] and PD control[2]. Serrarens, et al.[3] suppresses the stick slip motion by the frequency shaping of H_∞ control. H_∞ control is used by automatically shaping of the disturbance compensation and the (semi)complementary sensitivity function[4]. H_∞ loop shaping is a control system design method proposed by McFarlane, et al.[5]. The H_∞ loop shaping controller has a structure with LQ state feedback gain and state observer, so it is expected to improve the plant response using the evaluation function of the LQ control [6]. As an example of applying the positioning control system by the H_∞ loop shaping, Moon, et al.[7] design the controller that takes the disturbance control and the reference tracking performance into consideration.

1.2 Objectives and Method

In this study, we propose the method of the positioning control for the ball screw system achieved by H_∞ loop shaping. The designed controller satisfies the friction compensation, the reference tracking performance, and improvement of plant response by using weight functions. The dynamic weight function and the constant matrix are used. The dynamic weight function is selected to satisfy the friction compensation and the reference tracking performance. The friction compensation is focused on the frequency characteristics of the friction. The frequency region where a static friction and the stick-slip motion appears predominantly is identified. The constant weight is selected to improve the plant response. The selection of the constant weight for LQ control is easier than selecting appropriate weighting function for standard H_∞ control synthesis framework. Thus in this study, the constant weight is selected to simplified the trial and error for weight function. The effectiveness of the H_∞ loop shaping controller is illustrated by using the simulations with the nonlinear friction and the experiments.

2 Characteristics of Control Plant

2.1 Ball Screw System

In this study, the ball screw system is used as a control plant. It controls the table position using drive force of the DC servo motor(rated capacity 110[W], rated torque 0.221[Nm]) through the ball screw(entire length 100[mm]). The optical encoder(resolution performance 0.1[μm]) is used to measure the position.

2.2 Modeling of Plant

The motion equation is shown in Eq.(1), where y[m] is the position of the table position, $u(t)$ is the current input of the motor. Physical parameters are shown in Table 1.

$$M\ddot{y}(t) + F_v\dot{y}(t) = \frac{K_t}{R}u(t) \qquad (1)$$

Table 1　Parameters of ball-screw system

torque constant K_t	0.34[Nm/A]
coefficient of viscosity F_v	5.0×10^3[Ns/m]
mass of table M	0.49[kg]
ball screw constant R	6.37×10^{-4}[m/rad]

Let the state vector $x(t) = [y(t) \; \dot{y}(t)]^T$, the state space representation of the ball screw system described by Eq.(2). In this study, Eq.(2) is used by the control design.

$$\dot{x}(t) = \begin{bmatrix} 0 & 1 \\ 0 & -\frac{F_v}{M} \end{bmatrix} x(t) + \begin{bmatrix} 0 \\ \frac{K_t}{RM} \end{bmatrix} u(t)$$

$$x(t) = \begin{bmatrix} 1 & 0 \\ 0 & 1 \end{bmatrix} x(t) \qquad (2)$$

2.3 Modeling of Nonlinear Friction

Generally, the friction model is consisted of the static friction, the coulomb friction, and the viscous friction. Marton et al.[8] compensates the stick slip motion by using the friction model with the Striebeck effect. Thus in this study, the Tustin model[8], which is the nonlinear friction model with the Striebeck effect, is used. The Tustin model is shown in Eq.(3).

$$F_n = (F_c + (F_s - F_c)e^{-\frac{|\omega|}{\omega_s}}) \times \mathrm{sgn}(\omega) + F_v\omega \qquad (3)$$

Where ω is the table velocity, ω_s is the Striebeck velocity, F_s is the maximum static frictional force, F_c is the coulomb frictional force, F_v is the viscous friction coefficient, $\mathrm{sgn}(\cdot)$ is the signum function. The friction is identified by the response experiments which gives the sinusoidal input to the ball screw system. In this study, the nonlinear simulation is conducted by using the friction model of Eq.(3).

2.4 Characteristics of Nonlinear Friction

Even though the friction itself is nonlinear, the behavior of friction can be considered to have some frequency or repeatedly movement. In this study we try to extract some frequency that might explain the stick-slip motion. The stick-slip motion is analyzed by giving the current of 0.4[A] to the plant in open loop. The table position is shown in Fig.1, and its spectrum is shown in Fig.2. As can be seen in Fig.2, the stick-slip motion has some dominant frequency in near 10[rad/sec]. Thus in this study, the low frequency(0[rad/sec]) for static friction and near 10[rad/sec] for stick-slip are considered for friction compensation.
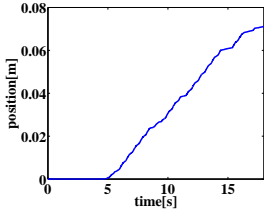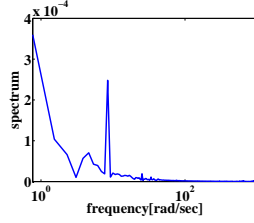
Fig. 1 Stick slip motion   Fig. 2 Spectrum

3 Design of Positioning Control

3.1 H_∞ Loop Shaping

The control design via H_∞ loop shaping proposed by McFarlane, et al.[5]. It is well known that the H_∞ loop shaping controller $C_\infty(s)$ for the design model $P_s(s) = \{A_d, B_d, C_d, D_d\}$ is given by Eq.(6) using the positive solution X and Z for Ricatti equations Eq.(4) and Eq.(5). λ_{max} is the maximum eigenvalue.

$$(A_d - B_d S^{-1} D_d^T C_d)^T X + X(A_d - B_d S^{-1} D_d^T C_d)$$
$$-XB_d S^{-1} B_d^T X + C_d^T R^{-1} C_d = 0 \quad (4)$$
$$(A_d - B_d S^{-1} D_d^T C_d)Z + Z(A_d - B_d S^{-1} D_d^T C_d)^T$$
$$-ZC_d^T R^{-1} C_d Z + B_d S^{-1} B_d^T = 0 \quad (5)$$
$$R = I + D_d D_d^T, S = I + D_d^T D_d$$

$$C_\infty(s) = \left[\begin{array}{c|c} A_d + B_d F + H(C_d + D_d F) & H \\ \hline B_d^T X & -D_d^T \end{array} \right] \quad (6)$$
$$F = -S^{-1}(D_d^T C_d + B_d^T X), L = (1 - \gamma^2)I + XZ,$$
$$H = \gamma^2 (L^T)^{-1} Z C_d^T, \gamma > (1 + \lambda_{max}(XZ))^{\frac{1}{2}}$$

The designed controller $C(s)$ decreases the effect from the friction δ and the reference input r to the control input u and the state x in the plant $P(s)$. Fig.3 shows the block diagram of $P(s)$ and $C(s)$. From Fig.3, the
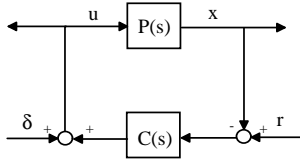

Fig. 3 Block diagram of the system

minimizing H_∞ norm problem of the transfer function matrix from δ, r to x, u is given by Eq.(7).

$$\left\| \left[\begin{array}{c} I \\ C(s) \end{array} \right] (I + P(s)C(s))^{-1} [I \ P(s)] \right\|_\infty < \gamma \quad (7)$$

H_∞ loop shaping controller which achieves the reference tracking performance and the friction compensation is designed by using the evaluation function Eq.(7).

3.2 Selection of Weight Functions

H_∞ loop shaping controller which improves the controlled performance is introduced by multiplying the weight functions to back and forth of the open loop transfer function. In this study, $W(s)$ and the constant matrix $Q^{\frac{1}{2}}$ are the weight functions shown in Fig.4(a). The plant $P(s)$ is extended by the weight functions $W(s)$ and $Q^{\frac{1}{2}}$. Then the controller $C_\infty(s)$ is synthesized for

the extended system $P_s(s) = Q^{\frac{1}{2}} P(s) W(s)$. Fig.4(b) is the equivalent transformation of Fig.4(a). Final controller $C(s) = W(s) C_\infty(s) Q^{\frac{1}{2}}$ is introduced by connecting $C_\infty(s)$ and the weight functions once again. In Fig.4,
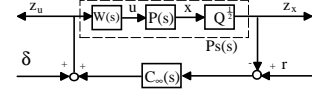
(a) Closed loop system
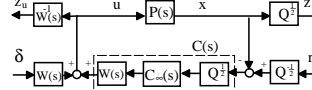
(b) Equivalent closed loop system

Fig. 4 H_∞ loop shaping method

the transfer function matrix from the external input $\{r, \delta\}$ to evaluation output $\{z_u, z_x\}$ is given by Eq.(8).

$$\begin{bmatrix} z_u \\ z_x \end{bmatrix} = \begin{bmatrix} P_{z_u r}(s) & P_{z_u \delta}(s) \\ P_{z_x r}(s) & P_{z_x \delta}(s) \end{bmatrix} \begin{bmatrix} r \\ \delta \end{bmatrix} \quad (8)$$
$$P_{z_u r}(s) = W^{-1}(s)(1 + C(s)P(s))^{-1} C(s) Q^{-\frac{1}{2}}$$
$$P_{z_u \delta}(s) = (1 + C(s)P(s))^{-1}$$
$$P_{z_x r}(s) = Q^{\frac{1}{2}} (I + P(s)C(s))^{-1} P(s)C(s) Q^{-\frac{1}{2}}$$
$$P_{z_x \delta}(s) = Q^{\frac{1}{2}} (I + P(s)C(s))^{-1} P(s) W(s)$$

Eq.(8) can be explained as follows. $P_{z_u r}(s)$ is not considered because of $Q^{-\frac{1}{2}} \simeq 0$ if the value of $Q^{\frac{1}{2}}$ is large. The control input is not influenced the disturbance by minimizing norm of $P_{z_u \delta}(s)$. $P_{z_x r}(s)$ is the closed loop transfer matrix. $P_{z_x \delta}(s)$ is the disturbance control characteristic, and the effect of the disturbance is minimized by using the constant matrix $Q^{\frac{1}{2}}$ and the dynamic weight function $W(s)$. Thus the selection of the weight function $W(s)$ and $Q^{\frac{1}{2}}$ influences the control performance widely. $W(s)$ is designed to satisfy the reference tracking performance and the friction compensation and $Q^{\frac{1}{2}}$ is selected to improve the plant response.

3.3 Selection of $W(s)$

From section 2.4, the ball screw system has the stick-slip motion in near 10[rad/sec] and the static friction in the low frequency region. Thus the gain of $W(s)$ is raised in the low frequency and near 10[rad/sec]. The final controller is given by $C(s) = W(s) C_\infty(s) Q^{\frac{1}{2}}$, so the controller that has the reference tracking performance is designed by adding the integrator to $W(s)$. In the result, $W(s)$ is given by Eq.(9) to raise the gain in the low frequency and close 10[rad/sec].

$$W(s) = \frac{10s + 10}{0.01s + 1} \times \frac{1}{s} \quad (9)$$

3.4 Selection of $Q^{\frac{1}{2}}$

The H_∞ loop shaping controller is improved the plant response by using the evaluation function of LQ control. Trial and error for H_∞ weight function is not clear compared with traditional LQ control synthesis. Thus in this study, the constant weight $Q^{\frac{1}{2}}$ is selected to simplified the trial and error for weight function. In

this ball screw system, the feedthrough term of the extended system is $D_d = 0$. Then the H_∞ loop shaping controller $C_\infty(s)$ is solved by two Riccati equations Eq.(10) and Eq.(11), where $P_s(s) = Q^{\frac{1}{2}}P(s)W(s) = \{A_d, B_d, C_d, D_d\}$.

$$A_d^T X + X A_d - X B_d B_d^T X + C_d^T C_d = 0 \quad (10)$$

$$A_d Z + Z A_d^T - Z C_d^T C_d Z + B_d B_d^T = 0 \quad (11)$$

From the solution of X and Z, the controller is given by Eq.(12), Eq.(13).

$$\dot{x}_k(t) = (A_d + B_d F + H C_d)x_k(t) + H y_k(t) \quad (12)$$

$$u_k(t) = F x_k(t) \quad (13)$$

Where $F = -B_d^T X, H = \gamma^2 W_1^{-T} Z C^T, W_1 = I + (XZ - \gamma^2 I)$. From Eq.(12) and Eq(13), the H_∞ loop shaping controller $C_\infty(s)$ can be considered as the output feedback controller consisting of a state feedback and observer. The block diagram of the closed loop system is shown in Fig.5. The state feedback gain F in Eq.(12)
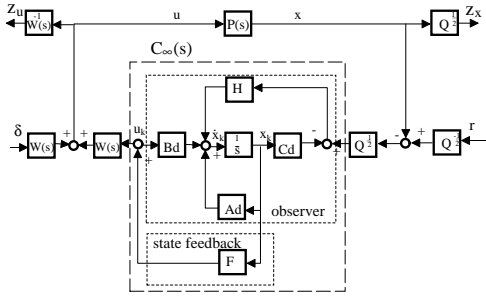

Fig. 5 Block diagram of $C_\infty(s)$

and Eq.(13) is given $F = -B_d^T X$, and X is the solution of the Riccati equation Eq.(10).

On the other hand, it is well known that the Riccati equation for Eq.(14) is given in Eq.(15), and the state feedback gain is $F = -B_d^T X$.

$$J = \int_0^\infty (x(t)^T Q x(t) + u(t)^T u(t))dt \quad (14)$$

$$A_d^T X + X A_d - X B_d B_d^T X + Q = 0 \quad (15)$$

When $z_x(t)$ is represented $z_x(t) = C_d x_d(t) = Q^{\frac{1}{2}} x(t)$, x_d is the state of $P_s(s)$. The evaluation function of Eq.(15) is equivalent to Eq.(16).

$$J = \int_0^\infty (x(t)^T Q x(t) + u(t)^T u(t))dt$$

$$= \int_0^\infty (z_x(t)^T z_x(t) + u(t)^T u(t))dt$$

$$= \int_0^\infty (x_d^T C_d^T C_d x_d(t) + u(t)^T u(t))dt \quad (16)$$

Thus the Riccati equation for Eq.(16) is equivalent to Eq.(10), and $F = -B_d^T X$ of Eq.(13) is the state feedback gain using LQ control. The state feedback gain F that minimizes the the evaluation function J is obtained. The selection of the constant weight $Q^{\frac{1}{2}}$ for LQ control is easier than selecting appropriate weighting function for standard H_∞ control synthesis framework. The constant weight $Q^{\frac{1}{2}}$ is given in Eq.(17).

$$Q^{\frac{1}{2}} = \begin{bmatrix} 4000 & 0 \\ 0 & 50 \end{bmatrix} \quad (17)$$

3.5 Characteristics of Disturbance Rejection

The characteristics of disturbance rejection and controller are analyzed by the gain diagram to verify the effectiveness of the weight functions. Fig.6 shows the gain diagram from the friction δ to the table position y. From Fig.6, the disturbance rejection is achieved in
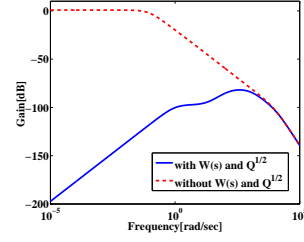

Fig. 6 Gain diagram from friction to output

the low frequency region and near 10[rad/sec]. This diagram shows the effectiveness of the proposed method. The obtained controller $C_\infty(s)$ is as follows.

$$C_\infty(s) = \begin{bmatrix} \frac{2.7\times10^3 s^3+2.9\times10^7 s^2+2.2\times10^{10} s+5.6\times10^{10}}{s^4+1.9\times10^4 s^3+1.0\times10^8 s^2+1.4\times10^{10} s+3.5\times10^{10}} \\ \frac{9.2\times10^3 s^3+9.7\times10^7 s^2+2.9\times10^{10} s+7.3\times10^{10}}{s^4+1.9\times10^4 s^3+1.0\times10^8 s^2+1.4\times10^{10} s+3.5\times10^{10}} \end{bmatrix} \quad (18)$$

The two dimensional controller is obtained by using the balanced truncation method[9] for $C_\infty(s)$.

$$C_{\infty 2}(s) = \begin{bmatrix} \frac{2.9\times10^2 s+2.0\times10^6}{s^2+1.0\times10^4 s+1.2\times10^6} \\ \frac{9.5\times10^2 s+2.6\times10^6}{s^2+1.0\times10^4 s+1.2\times10^6} \end{bmatrix} \quad (19)$$

The finally obtained controller $C(s) = W(s)C_{\infty 2}(s)Q^{\frac{1}{2}}$ is Eq.(20). The gain diagram of $C(s)$ is shown in Fig.7.

$$C(s) = \begin{bmatrix} C_1(s) \\ C_2(s) \end{bmatrix}$$

$$= \begin{bmatrix} \frac{1.0\times10^8 s^2+7.2\times10^{10} s+7.2\times10^{10}}{5.0\times10^{-2} s^4+5.5\times10^2 s^3+5.9\times10^4 s^2+9.7\times10^5 s} \\ \frac{5.5\times10^6 s^2+1.2\times10^9 s+1.2\times10^9}{5.0\times10^{-2} s^4+5.5\times10^2 s^3+5.9\times10^4 s^2+9.7\times10^5 s} \end{bmatrix} \quad (20)$$

As can be seen in Fig.7, the controller $C(s)$ is expected
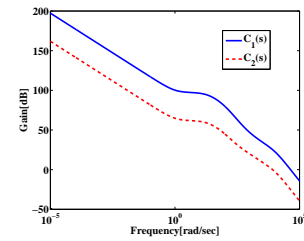

Fig. 7 Gain diagram of $C(s)$

to have the reference tracking performance and the friction compensation because the gain of $C(s)$ is risen in the low frequency region and near 10[rad/sec].

4 Simulations and Experiments

4.1 Step Response

The step response of the ball screw system is verified by simulations and experiments. The friction model shown in section 2.3 is used for the nonlinear simulations. The simulation and the experiment are conducted in the following cases to verify the effectiveness of the frequency shaping.

- Case 1 : $\hat{W}(s) = \frac{10}{s}$
(The same gain as Case 2 in the low frequency region)
- Case 2 : $W(s) = \frac{5s+10}{0.01s+1} \times \frac{1}{s}$

$\hat{W}(s)$ does not take account of the disturbance that causes the stick-slip motion near 10[rad/sec]. The simulation result of the table position[m] and the current input[A] are shown in Fig.8 and Fig.9, respectively. From
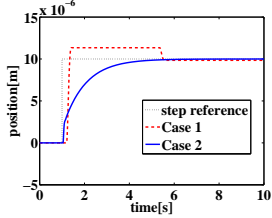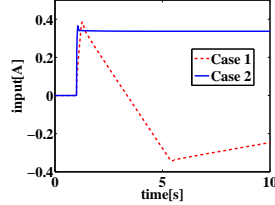
Fig. 8 Sim of output

Fig. 9 Sim of input

Fig.8, the step response in Case 1 follows the reference eventually by the integrator. However the overshoot is occurred by the friction. On the other hand, the step response in Case 2 follows the reference without stationary error and overshoot. As can be seen in Fig.9, the input is applied to reject the static friction at the rising moment. Thus the design controller achieved reference tracking performance and friction compensation. Then the experiment is run in the same condition of the simulation. The table position[m] is shown in Fig.10, and the control input[A] is shown in Fig.11.
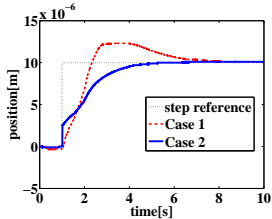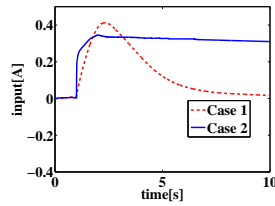
Fig. 10 Exp of output

Fig. 11 Exp of input

As can be seen in Fig.8 and Fig.10, there are some difference between the real friction and our friction model. However the experiment result has the same characteristics with the simulation. This mean that our friction model has a certain accuracy. Thus the precise simulation is achieved by getting the friction model used in section 2.3. From Fig.10, the step response in Case 2 follows the reference without the stationary error and the overshoot. As can be seen in Fig.11, the input is given to reject the static friction at the rising moment. The effectiveness of the proposed method is verified.

4.2 Ramp response

The ramp response of the ball screw system is verified by simulations and the experiments as well as the previous section. The simulation and the experiment conditions are the same as section 4.1. The simulation result of the table position[m] and the current input[A] are shown in Fig.12 and Fig.13, respectively. From Fig.12, the stick-slip motion is observed in Case 1. However the ramp response in Case 2 follows the reference without the stick slip motion. As can be seen in Fig.13, the input is given to reject the static friction at the rising moment. Based on the simulation result, the experiment is conducted in the same condition of the simulation. The table position is shown in Fig.14, and the control input
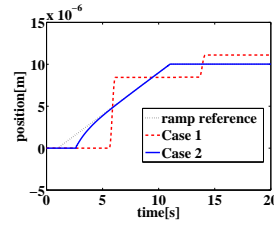
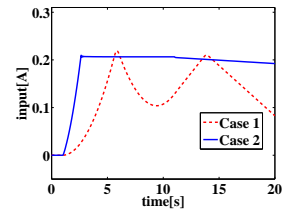Fig. 12 Sim of output

Fig. 13 Sim of input

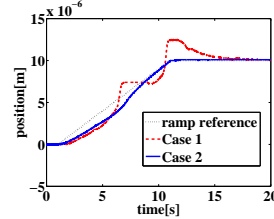is shown in Fig.15. There are some difference between
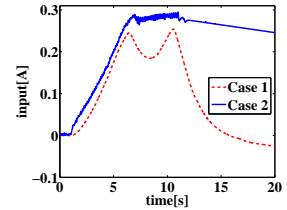
Fig. 14 Exp of output

Fig. 15 Exp of input

the real friction and friction model. However the experiment result has the same characteristics with the simulation. From Fig.14, the table position follows the reference without the stick slip motion. As can be seen in Fig.15, the input is given to reject the static friction at the rising moment. From the simulation and the experiment result, the H_∞ loop shaping controller compensates the stick slip motion by using $W(s)$

5 Conclusion

In this study, the H_∞ loop shaping controller, which satisfies the reference tracking performance and the friction compensate, is designed for the ball screw system. The static friction and the stick-slip motion near 10[rad/sec] are compensated by frequency shaping $W(s)$. Even though the framework of the proposed method is H_∞ control, the other weight $Q^{\frac{1}{2}}$ is easily selected, since the weight $Q^{\frac{1}{2}}$ is equivalent to the weight for the traditional LQ control framework. The effectiveness of the proposed method is illustrated by the simulations and the experiments.

References

[1] Choi Y, K Yang, W. K Chung, H. R Kim, I. H Suh: On the Robustness and Performance of Disturbance Observer for Second-Order Systems, IEEE Trans. Automatic Control,48-2,315/320(2003)

[2] Pierre E. Dupont: Avoiding Stick-Slip Through PD Control, IEEE Trans. Automatic Control, 39-5, 1094/1097(1994)

[3] A.F.A. Serrarens, M.J.G. van de Molengraft, J.J. Kok, and L. van den Steen: H_∞ Control for Suppressing Stick-Slip in Oil Well Drillstrings, IEEE Control Systems, 18-2, 19/30(1998)

[4] Tsutomu Mita, Mitsuo Hirata, Zhang Hui, Kenichi Murata: H_∞ Control Versus Disturbance-Observer-Based Control, IEEE Trans. Industrial Electronics, 45-3, 488/495(1998)

[5] D McFarlane, K Glover: A Loop Shaping Design Procedure Using H_∞ Synthesis, IEEE Trans. Automatic Control, 37-6, 759/769(1992)

[6] Ryoji Kawatani, Hirohide Matsushima: Robust Vibration Control of a Flexible Bridge Using Normalized Coprime Factorization Approach, Transactions of ISCIE,6-1,48/56(1993),in Japanese.

[7] J Moon,C.W Lee, C. C Chung Y. S Kim: Design of Disturbance Observer via the Robust Stabilization and Loop Shaping Methods, IEEE Trans. Automatic Control, 17-1, 9272/9277(2008)

[8] Lorinc Marton,Bela Lantos: Modeling, Identification, and Compensation of Stick-Slip Friction, IIEEE Trans. Industrial Electronics, 54-1, 511/521(2007)

[9] K Zhou, J Doyle, K Glover: Robust and Optimal Control, Prentice-Hall, Inc.,1996